DOI 10.5012/bkcs.2011.32.5.1527

Interaction of Gas-phase Atomic Hydrogen with Chemisorbed Oxygen Atoms on a Silicon Surface

Sang Kwon Lee, Jongbaik Ree,[*] Yoo Hang Kim,[†] and Hyung Kyu Shin[‡]

Department of Chemistry Education, Chonnam National University, Kwangju 500-757, Korea. [*]E-mail: jbree@chonnam.ac.kr
[†]Department of Chemistry and Center for Chemical Dynamics, Inha University, Incheon 402-751, Korea
[‡]Department of Chemistry, University of Nevada, Reno, Nevada 89557, U. S. A.
Received December 24, 2010, Accepted March 9, 2011

The reaction of gas-phase atomic hydrogen with oxygen atoms chemisorbed on a silicon surface is studied by use of the classical trajectory approach. We have calculated the probability of the OH formation and energy deposit of the reaction exothermicity in the newly formed OH in the gas-surface reaction H(g) + O(ad)/Si → OH(g) + Si. All reactive events occur in a single impact collision on a subpicosecond scale, following the Eley-Rideal mechanism. These events occur in a localized region around the adatom site on the surface. The reaction probability is dependent upon the gas temperature and shows the maximum near 1000 K, but it is essentially independent of the surface temperature. The reaction probability is also independent upon the initial excitation of the O-Si vibration. The reaction energy available for the product state is carried away by the desorbing OH in its translational and vibrational motions. When the initial excitation of the O-Si vibration increases, translational and vibrational energies of OH rise accordingly, while the energy shared by rotational motion varies only slightly. Flow of energy between the reaction zone and the solid has been incorporated in trajectory calculations, but the amount of energy propagated into the solid is only a few percent of the available energy released in the OH formation.

Key Words : Classical trajectory, Silicon, Hydrogen, Oxygen, OH

Introduction

In recent years much work has been devoted to the investigation of the physical properties and chemical reactivities of atoms and molecules adsorbed on solid surfaces.[1-3] Such works have produced valuable information about the chemical and physical properties of adsorbed layers, and this information is essential for the development of fundamental concepts on gas-surface reactions. An important part of this development is understanding the mechanisms of such reactions. In gas-adatom interactions taking place on a solid surface, important reactive events involve the dissociation of the adatom-surface bond and association of the gas atom with the desorbing adatom. Thus the dynamics of energy flow between the gas-adatom interaction and the adatom-surface vibration, adatom-surface bond dissociation, and gas-adatom bond formation are problems of fundamental importance in understanding the details of such reactions. Such reactions are often highly exothermic, so there is a large amount of energy to be deposited in the various motions of the product.[4-11] The characterization of time evolution of such reactive events and energy disposal in the product is important in elucidating the mechanistic details. Furthermore, such reactions can produce active surface sites, which can subsequently react with incident or pre-adsorbed molecules or atoms. While the reactions taking place on a metallic surface are important on studying catalysis, those occurring on a silicon surface are of importance in the processing of silicon-based materials.[10-15]

The purpose of this paper is to study the dynamics of gas-phase atomic hydrogen with chemisorbed oxygen atoms on silicon (001)-(2×1) with particular emphasis on the disposal of the reaction exothermicity. In this reaction, the difference between the exothermicity of the gas-phase reaction and the heat of chemisorption is significant, and the activation energy is known to be very low (≈ 2 kcal/mol).[16-18] These characteristics coupled with the unusual kinematics associated with the reaction of a light atom with a heavy adatom-surface system dominate the ER dynamics of this reaction. We will use a modified version of the London-Eyring-Polanyi-Sato (LEPS) procedure, which includes additional energy terms that result from the participation of adjacent surface sites in the hydrogen-to-surface interaction,[10] for the potential energy surface and use it in the molecular time scale generalized Langevin equation (MTGLE), which is designed to describe the combined motions of reaction-zone atoms and surface atoms.[19] The incorporation of surface atom dynamics enables us to determine the flow of energy between the reaction zone and the solid in an accurate way. We consider the reaction taking place in the gas temperature range of 300-2500 K and surface temperature range of 0-700 K.

Model

The interaction model and numerical procedures have already been reported in Ref. 10. We briefly summarize the essential aspect of the model for the interaction of atomic

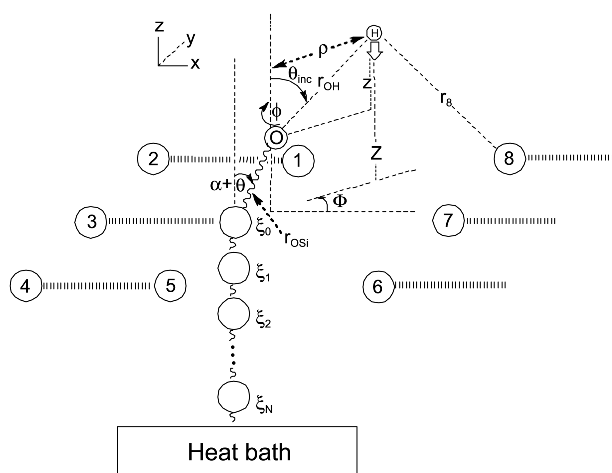

Figure 1. Interaction model. The zeroth atom on which O is adsorbed is surrounded by eight adjacent Si atoms. The N-atom chain connects the O-Si vibration to the heat bath. The coordinates (r_{OSi}, θ, ϕ) for O, (ρ, Z, Φ) for H, and ξ's for the N chain atoms are defined. α is the tilt angle, r_{OH} is the O to H distance, and r_i is the H to the ith surface-layer Si distance (only r_8 is indicated).

hydrogen with O chemisorbed on the Si(001)-(2×1) surface reconstructed by dimer formation along the [110] direction. For easy reference we display the collision model in Figure 1 defining the pertinent coordinates. The O atom is chemisorbed on the Si atom of the symmetric dimer structure. This adatom site, which is surrounded by eight adjacent Si atom, is the $N = 0$ member of the ($N + 1$)-atom chain, which links the reaction zone to the heat bath. We shall refer to this adatom site as the zeroth Si atom. Thus, in addition to the adatom, the incident atom is in interaction with all these $8 + (N + 1)$ Si atoms, where the zeroth atom on which the oxygen atom is chemisorbed, is surrounded by eight surface-layer Si atoms and the last (Nth) atom is bound to the bulk phase. The atoms of the semi-infinite collinear lattice are labeled 0, 1, 2, 3, ..., all having mass M_s with the instantaneous displacement of the ith atom from its equilibrium position denoted by ξ_i. In general, the real solid is three dimensional, non-nearest neighbor coupled, and anharmonic. Thus our model oversimplifies the real solid and cannot explain the phonon spectrum, but it is based on an intuitive picture of the easy flow of energy through a nearest neighbor along the harmonic chain. The extent of energy flow is crucial to understanding gas-surface reactivity, in particular the extent of product excitation. If more solid atoms are included in modeling, there will be an increase in energy flow to the solid.[20] However, the general trends are not changed significantly.

All these interaction energy terms are included in a modified version of the LEPS potential energy surface. Since the gas atom-to-nine surface atom distances have the functional dependence $r_i \equiv r_i(r_{OSi}, \theta, \phi, \rho, Z, \Phi)$ and the H(g)-to-O(ad) distance $r_{OH} \equiv r_{OH}(r_{OSi}, \theta, \rho, Z)$, we can obtain the potential energy $U(r_{OSi}, \theta, \phi, \rho, Z, \Phi, \{\xi\})$, where $\{\xi\}$ is the collective notation for ($\xi_0, \xi_1, ..., \xi_N$) denoting the vibrational coordinates of the ($N + 1$)-chain atoms. Here, we have transformed the coordinate of the incident gas atom (x_H, y_H, z_H) into the cylindrical system (ρ, Z, Φ) and the adatom coordinate (x_O, y_O, z_O) into (r_{OSi}, θ, ϕ). Prior to dissociation, the restricted motion of the adatom around its equilibrium position from Si will be described by the tilt angle α and hindered rotational angles θ and ϕ. We take $\alpha = 20^o$, which is very close to the 19.5° that represents the tetrahedral geometry (109.5°-90.0°).[18]

Each Coulomb or exchange term of the LEPS potential function contains the Sato parameter (Δ). By varying their values systematically, we find the Sato parameters which best describe the desired features of minimizing barrier height and attractive well depth in both the entrance and exit channels. They are $\Delta_{OH} = 0.11$, $\Delta_{OSi} = 0.08$, and $\Delta_{HS} = 0.37$ for the hydrogen-to-nine surface-layer Si atom interactions. We find the barrier height of 1.04 kcal/mol for H(g) + O(ad)/Si. In a related system of H(g) + Cl(ad)/Si, the observed activation energy is 2.1 ± 0.2 kcal/mol.[7]

To study the reactive event, we follow the time evolution of the reaction system by integrating the equations of dynamics, which describe the motions of the reaction-zone atoms and N-chain atoms. An intuitive way to treat the dynamics of the reaction involving many surface atoms is to solve the motions of primary zone atoms governed by the MTGLE set of the equations for the gas atom, adatom, zeroth Si atom and N chain atoms. The equations of motion for the gas atom and adatom are in the form

$$m_j \ddot{Y}_j(t) = -\partial U(r_{OSi}, \theta, \phi, \rho, Z, \Phi, \{\xi\})/\partial Y_j \quad (1)$$

where $j = 1, 2, ..., 6$ for Z, ρ, Φ, r_{OSi}, θ, ϕ, with $m_1 = m_H$, $m_2 = \mu_{OH}$, $m_3 = I_{OH}$, $m_4 = \mu_{OSi}$, and $m_5 = m_6 = I_{OSi}$. Here μ is the reduced mass and I is the moment of inertia. The potential energy contains the effects of all surface-layer atoms. For the ($N + 1$)-atom chain dynamics, we have[19,20]

$$\ddot{\xi}_0(t) = -\omega_{e,0}^2 \xi_o(t) + \omega_{c,1}^2 \xi_1(t) - M_s^{-1} \partial U(r_{OSi}, \theta, \phi, \rho, Z, \Phi, \{\xi\})/\partial \xi_0 \quad (2a)$$

$$\ddot{\xi}_1(t) = -\omega_{e,1}^2 \xi_1(t) + \omega_{c,1}^2 \xi_0(t) + \omega_{c,2}^2 \xi_2(t) \quad (2b)$$

$$\ddot{\xi}_j(t) = -\omega_{e,j}^2 \xi_j(t) + \omega_{c,j}^2 \xi_{j-1}(t) + \omega_{c,j+1}^2 \xi_{j+1}(t), \quad j = 1, 2, .., N-1 \quad (2c)$$

$$\ddot{\xi}_N(t) = -\Omega_N^2 \xi_N(t) + \omega_{c,N}^2 \xi_{N-1}(t) - \beta_{N+1} \dot{\xi}_N(t) + f_{N+1}(t) \quad (2d)$$

In these equations, M_s is the mass of the silicon atom, ω_e the Einstein frequency, ω_c the coupling frequency characterizing the chain, and Ω_N the adiabatic frequency. The quantity f_{N+1}(t) determines the random force on the primary system arising from thermal fluctuation in the heat bath. The friction coefficient β_{N+1} is very close to $\pi\omega_D/6$, where ω_D is the Debye frequency.[19] The Debye temperature of Si is 640 K.[21] All values of the frequencies and friction coefficients are presented elsewhere.[22] The initial conditions needed to solve these equations have already been given in earlier papers.[18]

The numerical procedures include an extensive use of Monte Carlo routines to generate random numbers for initial conditions. The first step is to sample collision energies E

from a Maxwell distribution at the gas temperature T_g and to weigh the initial energy of O(ad)-Si_0 and all chain atom vibrations by a Boltzmann distribution at the surface temperature T_s. The normal component of the incident energy is $E\cos^2\theta_{inc}$, which will be used in solving the equations of motion, where $\theta_{inc} = \tan^{-1}(\rho/z)$ and $z = Z - r_{OSi}\cos(\alpha + \theta)$. In sampling impact parameters b, we note that the distance between the oxygen atoms adsorbed on the nearest sites is 3.79 Å. Thus we take the half-way distance so that the flat sampling range is $0 < b < 1.89$ Å (i.e., b_{max} = 1.89 Å). In the collision with $b > 1.89$ Å, the gas atom is now in the interaction range of the oxygen atom adsorbed on the adjacent surface site or in that of the bare surface site. Also sampled are the initial values of θ, ϕ, and Φ. The initial conditions for $(N+1)$-chain atom vibrations at surface temperature T_s are

$$\xi_j(t_0) = A_j \sin(\omega_{ej} t_0 + 2\pi\delta_j) \tag{3a}$$

$$\dot{\xi}_j(t_0) = \omega_{ej}[A_j^2 - \xi_j(t_0)^2]^{1/2} \tag{3b}$$

where $A_j^2 = 2kT_s/M\omega_{cj}^2$ and $2\pi\delta_j$ is the initial phase of the vibration of jth solid atom, in which δ_j are mutually random numbers with flat distribution in the closed interval (0, 1), and j = 0, 1, 2, ..., N. For the $(N+1)$ silicon atoms, we thus need to sample $(N+1)\delta$'s.

Thus, each trajectory is generated with the set (E, b, $E_{OSi,0}$, θ_0, ϕ_0, Φ_0, $\{\xi\}_0$), where $\{\xi\}_0$ represents the initial values of $\{\xi\} = \{\xi_0, \xi_1, \ldots, \xi_N\}$. We sample 40,000 sets for each ensemble. We follow each trajectory for 50 ps, which is a sufficiently long time for OH(g) to recede from the influence of surface interaction, to confirm the occurrence of a reactive event forming OH. Furthermore, we confirm that each trajectory can be successfully back-integrated in the computational procedure. We take the chain length of $N = 10$.[18] All pertinent interaction and spectroscopic constants[23-28] used in the calculation are listed in Table 1.

Results and Discussion

The main topics to be considered in the present study are the probabilities of OH formation and amounts of energy deposited in the various motion of the product molecule OH. As mentioned above, we consider the reaction taking place in the gas temperature range of 300-2500 K and surface temperature range of 0-700 K. The results presented are mainly at T_g = 1800 K and T_s = 300 K. Even though the fraction of O-Si in the ground state is $f(v_{OSi} = 0) = 1 - e^{-\hbar\omega_{OSi}/kT}$ = 0.991 at this surface temperature, we have calculated the probabilities of OH formation and amounts of energy deposited in the product molecule OH with the fixed initial excitation of the v_{OSi} = 0, 1, 2, and 3, respectively. Nearly all reactive events of 40,000 trajectories sampled occur on the time scale less than 0.3 ps.

Table 1. Interaction Parameters for O(g) + H(ad)/Si

Interaction (i)	O-H	O-Si	H-surface
$D_{0,i}^0$ (eV)[a]	4.392	3.82	0.0433
ω_i (cm^{-1})[b]	3738	972	-
d_i (Å)[c]	0.9697	1.709	3.38
a_i (Å)[d]	0.2178	0.187	0.4

[a]$D_i = D_{0,i}^0 + ½\hbar\omega_i$ (ref. 23 for O-H; ref. 24 for O-Si; refs. 25 and 26 for H-Si). [b]Ref. 23 for O-H; The O-Si value 972 cm^{-1} is the average of the observed values lying between 965-980 cm^{-1} (refs. 27 and 28). [c]Ref. 23 for O-H; ref. 24 for O-Si; ref. 25 for H-Si. [d]The range parameters that enter in the Morse form of the LEPS function; $a_i = (D_i/2\mu_i)^{1/2}(1/\omega_i)$.

Reaction Probabilities. In Figure 2, we show the dependence of the reaction probability $P(T_g, T_s; b)$ on the impact parameter for the OH formation at the thermal condition of (T_g, T_s) = (1800, 300 K). This b dependence provides useful information about the region where OH formation occurs. As shown in Figure 2, the OH formation probability takes its maximum value at $b \approx 0$ and then decreases smoothly as b increases. At b = 0.2 Å, it is about 0.5 and the reaction ceases near b = 0.5 Å. The reaction occurs in a localized region around the adatom site on the surface. Such localized reactivity has been observed in the bromine and chlorine abstraction reactions on silicon by gas-phase atomic hydrogen.[18,29] On the other hand, in the O + H/Si system, the OH formation occurs in the range of $0 < b < 1.5$ Å collisions, where its $P(b)$ rises rapidly from a small value at b = 0 to the maximum value of 0.546 at b = 0.63 Å.[30] This striking difference is due to the fact that the energy transfer mechanism in the O + H/Si system is through the heavy-light-heavy atoms (**H-L-H**), while in the H + O/Si system it is through the **L-H-H** atoms. Because the adatom is tilted, the b = 0 collision in a three-dimensional collision does not represent the collinear configuration of H···O–Si. Therefore, the b = 0 collision is not the most efficient configuration for flow of energy between the loosely bound H···O bond and H-Si bond in the short-lived O···H-Si collision complex in the O + H/Si system.

In the **H-L-H** system collinearity plays an important role in energy transfer, but the kinetic energy of the incident particle plays a more important role in the **L-H-H** system. That is, the energy transfer shows the maximum at $\theta = 0°$

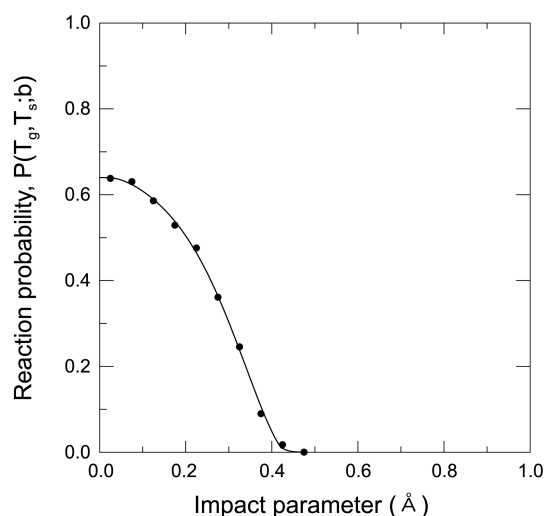

Figure 2. Dependence of the OH formation on the impact parameter at (1800, 300 K).

since $E_{inc} = E_k\cos^2\theta$.

As mentioned above, the OH formation occurs in the range of $0 < b < 1.5$ Å for the O + H/Si system whereas the OH formation occurs in $0 < b < 0.5$ Å for the H + O/Si system. The reactive reactions occur in the much narrower region for the H + O/Si system. This fact also supports the more important role played by the kinetic energy of the incident particle rather than the collinearity. From the *b*-dependent reaction probability we obtain the total reaction cross section of 0.177 Å^2 using the expression defined as $\sigma = 2\pi\int_0^{b_{max}} P(T_g, T_s; b)\, b\, db$, where b_{max} is 1.89 Å. The total cross section is small, in part reflecting the occurrence of reactive events in the immediate neighborhood of the adatom and a small value of the reaction probability.

The formation of OH occurs on a subpicosecond time scale through a single gas-surface collision. The ensemble average of reaction times is 0.15 ps. In Figure 3, we show the dependence of distribution of reaction times on the angle Φ, the azimuthal angle for H(g) on the surface plane. Reactive events are highly concentrated in the region of reaction times from 0.1 to 0.2 ps. Such a short time scale supports the occurrence of OH formation in a direct collision-induced pathway via an Eley-Rideal (ER) mechanism. The distribution also shows no particular preference in the direction of approach of H(g) to the surface in producing a reactive event.

In Figure 4(a), we show the reaction probability of the OH formation as a function of the surface temperature form 0 to 700 K at $T_g = 1800$ K. Over the surface temperature range, calculated reaction probabilities remains close to 0.09. The magnitude of the reaction probability is comparable to that of the atomic hydrogen abstraction reactions in H(g) + H(ad)/Si and O + H/Si systems.[26,30] This very weak temperature dependence suggests that the driving force for the oxygen abstraction reaction resides in the high potential energy of atomic hydrogen, as mentioned above. It is interesting to note that although the mass distributions are different, the basic energetics of these two reactions are very similar. As

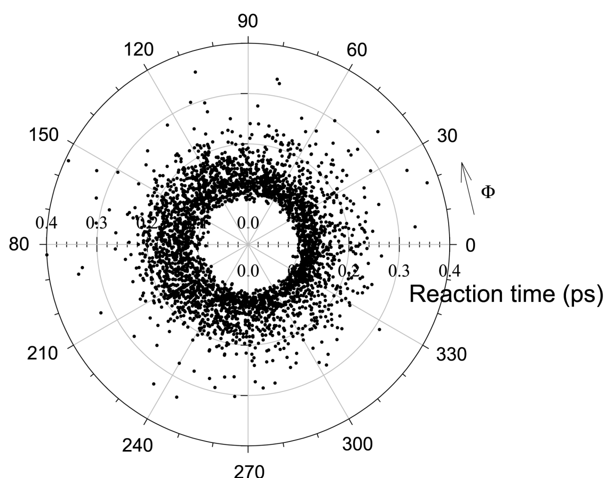

Figure 3. Distribution of reaction times. Plotted are reaction times of all OH forming events as a function of Φ. The $\Phi = 0^o$ line is the direction from the zeroth Si to the seventh Si, see Figure 1(b).

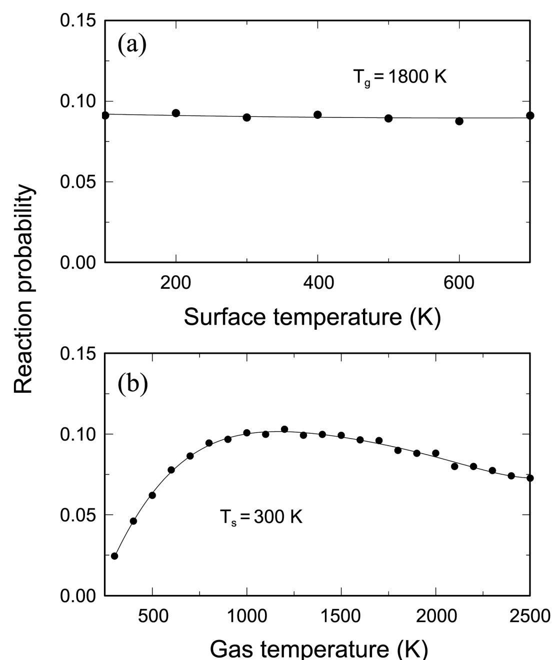

Figure 4. Dependence of the reaction probability $P(T_g, T_s)$ on the surface and gas temperatures. (a) Dependence on the surface temperature for the gas temperature fixed at 1800 K and (b) dependence on the gas temperature for the surface temperature fixed at 300 K.

noted above, for the adatom-surface interactions O(ad)/Si and H(ad)/Si, the dissociation energies are $D^0_{0,OSi} = 3.82$ eV and $D^0_{0,HSi} = 3.50$ eV, which are close to each other. Figure 4(a) shows that the effect of surface temperature on the reaction is negligible, which is a typical result for an ER process.

In all calculations, we have sampled the initial energy of the O-Si vibration, $E^0_{v,OSi}$, corresponding to quantum numbers $v_{OSi} = 0, 1, 2, ...$, weighted by a Boltzmann distribution. The contribution coming from higher vibrational states ($v_{OSi} > 0$) is only important at higher surface temperatures (>3000 K). At (1800, 300 K), the values for (T_g, T_s) for $v_{OSi} = 0$, 1, 2, and 3 are 0.0902, 0.0906, 0.0908, and 0.0909, respectively, showing a very weak dependence on the initial excitation of the adatom-surface vibration. When the Boltzmann population of initial vibrational states is used, the contribution coming from excited O-Si vibrational states is not important in the present system, since essentially all of the O-Si vibrations are in the ground state. For example, at $T_s = 300$ K, the fractions of the O-Si vibration in $v_{OSi} = 0$, 1, 2 are 0.9905, 0.0094, and 0.0001, respectively.

The dependence of the reaction probability on the initial excitation of the O-Si vibration is significantly different from the O(g) + H(ad)/Si system,[30] where increasing the initial vibrational state of the adsorbate from $v = 0$ to $v = 1$ increases the reaction probability nearly 20%.[11] The latter reaction involves the heavy-light-heavy (**H-LH**) mass distribution whose kinematics is very different from the present (**L-HH)** distribution despite the similar energetics as noted above. In the present case, the light atom approaches

the heavy adatom to the near normal gas-adatom equilibrium separation [see Figure 2], but its further approach to the surface is countered by the heavy adatom and energy flow between the adatom-surface vibration and the gas-adatom interaction becomes less efficient than that in the **H + LH** case. It is noteworthy that such energy flow blockage by the heavy atom has already been noted in the both experimental studies[31-33] and theoretical calculations.[34-37]

The dependence of the reaction probability on the gas temperature is much stronger than the T_s dependence shown in Figure 4(a). The results presented in Figure 4(b) for a fixed surface temperature 300 K shows the reaction probability rising rapidly with the gas temperature in the range of T_g = 300 to 1000 K, beyond which it decreases slightly with increasing temperature. The same trend was found in H + Cl/Si and H + Br/Si systems too.[18,29] The variation of reaction probability at lower temperatures follows a "normal" thermal effect that the extent of a chemical reaction increases with increasing temperature, but at higher temperatures, where high energy collisions dominate, the fast moving gas atom does not stay on the surface long enough to allow reaction. Thus, at high temperature, many trajectories leave the surface without reaction resulting in lower reaction probability.

Product Energy Distribution. The energy available for OH and the surface after the adatom-surface bond dissociation is ($\Delta D_0^0 + E_{OSi}^0 + E$) eV, where E_{OSi}^0 is the initial energy of the adatom-surface vibration and E is the hydrogen atom kinetic energy. The reaction exothermicity ΔD_0^0 is the difference between the O-Si dissociation energy and the OH dissociation energy. From the dissociation energies listed in Table 1, we find ΔD_0^0 = 0.572 eV for this exothermic reaction. In Table 2, we summarize the distribution of the ensemble-averaged energies deposited in OH as well as that propagated into the solid for v_{OSi} = 0, 1, 2 and 3. The calculation of the energy deposited in OH from the computer output is straightforward. The translational energy is $E_{trans,OH} = \frac{1}{2} m_{OH} (\dot{Z} - \gamma_H \cos\theta_{inc} \dot{r}_{OH})^2$, where $m_{OH} = (m_O + m_H)$ and $\gamma_H = m_H/(m_O + m_H)$. The rotational energy is $E_{rot,OH} = L_{OH}^2 / 2\mu_{OH} r_{OH}^2$, where the angular momentum $L_{OH} = \mu_{OH}(z\dot{\rho} - \rho\dot{z})$ with the corresponding quantum number $J_{OH} = L_{OH}/\hbar$. The equation for the OH vibrational energy takes the usual expression

Table 2. Distribution of the Reaction Exothermicity at T_g = 1800 and T_s = 300 K. The ensemble-averaged energies are in eV

v_{OSi}	$\langle E_{vib,OH} \rangle$	$\langle E_{tran,OH} \rangle$	$\langle E_{rot,OH} \rangle$	$\langle E_{s,OH} \rangle$
0	0.397	0.504	0.006	0.029
1	0.433	0.526	0.007	0.048
2	0.470	0.550	0.008	0.066
3	0.514	0.571	0.009	0.088

$E_{vib,OH} = \frac{1}{2}\mu_{OH}\dot{r}_{OH}^2 + D_{OH}[1 - e^{(r_{OH,e} - r_{OH})/2a}]^2$, where a is the range parameter and $r_{OH,e}$ is the equilibrium value of r_{OH}. The expression for the energy propagated from the reaction zone into the solid through the (N + 1)-atom chain is[18]

$$E_{s,OH} = \frac{1}{2} M_s \sum_{i=0}^{N} \dot{\xi}_i^2(t) + \frac{1}{2} M_s \sum_{i=0}^{N-1} \omega_{e,i}^2 \xi_i^2(t) + \frac{1}{2} M_s \Omega_N^2 \xi_N^2(t) + M_s \sum_{i=0}^{N-1} \omega_{c,i+1}^2 \xi_i(t) \xi_{i+1}(t).$$

We average all these energies over the ensemble of reactive trajectories to obtain the quantities $\langle E_{vib,OH} \rangle$, $\langle E_{trans,OH} \rangle$, $\langle E_{rot,OH} \rangle$ and $\langle E_{s,OH} \rangle$. For v_{OSi} = 0, the energies deposited in the vibrational, translational and rotational motions of OH are $\langle E_{vib,OH} \rangle$ = 0.397 eV, $\langle E_{trans,OH} \rangle$ = 0.504 eV, and $\langle E_{rot,OH} \rangle$ = 0.006 eV. The amount of energy propagated into the solid $\langle E_{s,OH} \rangle$ is only 0.029 eV. Thus, the gas-phase product OH carries away about 97% of the energy released in the reaction. Furthermore, 96% of the available energy deposits in the translational and vibrational motions. This type of product energy distribution with a major portion depositing in translation and vibration is characteristic of an ER mechanism.[9,38] Increasing the initial vibrational state of the adatom-surface vibration from v_{OSi} = 0 to 1, 2, and 3 causes a large increase in the OH vibrational and translational energies, while the energy of rotational motion changes very slightly.

When the initial vibrational state of the adsorbate is raised from v_{OSi} = 0 to 1, corresponding to the increase of initial vibrational energy by 0.120 eV, the ensemble-averaged energy deposited in the OH vibration increases from $\langle E_{vib,OH} \rangle$ = 0.397 to 0.433 eV, an increase of 0.036 eV. The ensemble-averaged energy deposited in the OH translation, $\langle E_{trans,OH} \rangle$ increases 0.027 eV, whereas the ensemble-averaged amount of energy propagated into the solid, $\langle E_{s,OH} \rangle$ increases

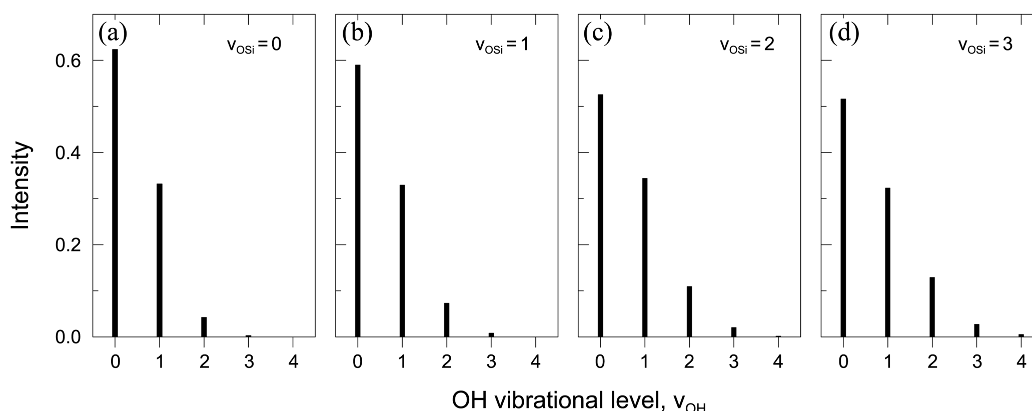

Figure 5. Vibrational population distribution of OH.

0.025 eV. A similar increase is seen when v_{OSi} rises from 1 to 2 and 2 to 3. There are other sources of energy, which can contribute to the newly formed OH bond, but the main contributor to the vibrational energy of OH is from OSi through the V→V energy transfer pathway. We note that the incident atom carries a significant amount of the collision energy, but its transfer to the nascent vibration is not efficient, i.e., a collision-induced T→V energy transfer process in this gas-surface reaction is inefficient.

In Figure 5, we show the vibrational population. Here the distribution is determined by assigning the quantum number v_{OH} determined as $v_{OH} = \text{int}[E_{vib,OH}/E_{vib}(v_{OH})]$, the integer nearest to the ratio $E_{vib,OH}/E_{vib}(v_{OH})$. Here $E_{vib}(v_{OH})$ is the vibrational energy determined from the eigenvalue expression $E_{vib}(v_{OH})/hc = \omega_e(v_{OH} + ½) - \omega_e x_e(v_{OH} + ½)^2$ with $\omega_e = 3737.76$ cm^{-1} and $\omega_e x_e = 84.881$ cm^{-1}.[25] For $v_{OSi} = 0$, the intensity of vibrational population for $v_{OH} = 1$ is 0.332 compared with 0.623 for $v_{OH} = 0$ (or the $v_{OH} = 1$ to $v_{OH} = 0$ population ratio 0.533). The $v_{OH} = 1$ population is significantly larger than that predicted by the Boltzmann distribution, thus representing the occurrence of a substantial vibrational excitation. Even at 1800 K, the Boltzmann distribution gives the fractions $f(v_{OH} = 0) = 1 - e^{-\hbar\omega/kT} = 0.950$ and $f(v_{OH} = 1) = [1 - e^{-\hbar\omega/kT}]e^{-\hbar\omega/kT} = 0.0478$, i.e., $f(v_{OH} = 1)/f(v_{OH} = 0)$ is only 0.050, so the vibrational population distribution of OH produced on the silicon surface seriously deviates from the prediction of the Boltzmann distribution law. The population of OH with the vibrational energy corresponding to $v_{OH} > 1$ increases slightly as the initial excitation of OSi increases, even though the reaction probability itself remains essentially unchanged as mentioned above. For example, for $v_{OSi} = 3$, the $v_{OH} = 1$ to $v_{OH} = 0$ population ratio is as large as 0.625. For this initial excitation, we find the formation of OH even in an excited state as high as $v_{OH} = 5$, although the population intensity is only 0.0003 (not shown in Figure 5).

Representative Trajectory. In Figure 6(a), we plot the time evolution of O-H, and O-Si distances for a representative case at (1800, 300 K). The time evolution of the O-H and O-Si distances clearly show the O-H bond formation and the O-Si bond dissociation. Note that after the H atom reaches the closest distance on impact, the O-Si distance begins to diverge, whereas the O-H distance undergoes a highly organized vibrational motion near the equilibrium bond distance $r_e = 0.9697$ Å. This vibrational motion clearly indicates the formation of a stable product molecule. In this case, the displacement of the O-Si bond distance from its equilibrium reaches 5 Å at $t = 0.17$ ps, at which time OH is formed.

The incident gas atom with collision energy E undergoes inelastic interaction with the adatom-surface vibration through the repulsive part of the H to O potential. This is an important process which produces energy exchange between the H to O interaction and the O-Si vibration. In order for the H atom to form O-H bond on a short-time scale, it must redirect its energy along the reaction coordinate in the early stage of collision. This energy is the primary driver for the reaction and the redirection occurs in the presence of strong attraction between H and O. When the H to O interaction

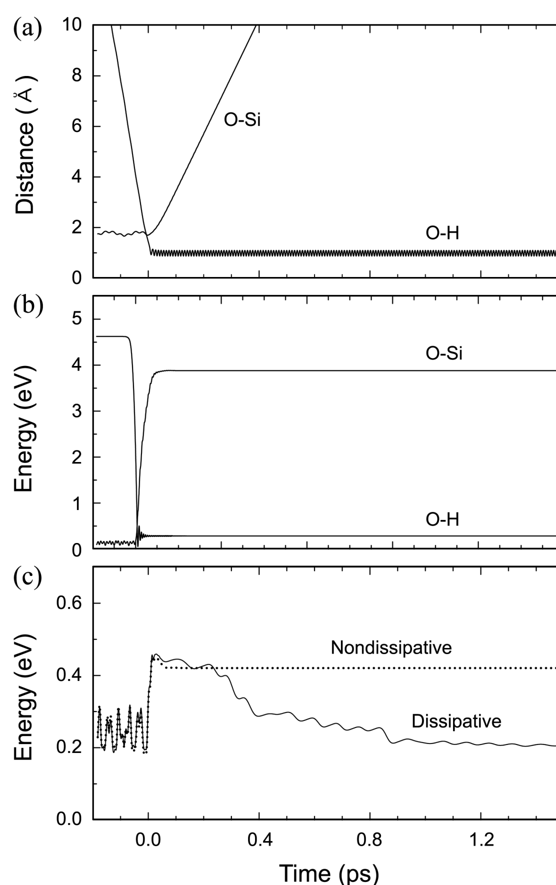

Figure 6. Dynamics of the representative trajectory at (1800, 300 K). (a) Time evolution of the O-H and O-Si distances. (b) Time evolution of the O-H and O-Si interaction energy. (c) Time evolution of the surface energy $E_s(t)$. The dotted curve represents the energy obtained assuming the absence of dissipation mechanism.

loses energy to the O-Si vibration, the incident gas atom falls into the O-H potential well. The high efficiency of this energy transfer process is evident in Figure 6(b), where the H to O interaction energy decreases sharply from D_{OH} to the final value $E_{v,OH(\infty)} = 0.285$ eV, whereas the O-Si vibrational energy, $E_{v,OSi}(t)$, rises rapidly from its initial value $E^0_{v,OSi}$ toward the dissociation threshold $D_{OSi} = 3.82$ eV. The comparison of the curves shown in Figures 6(a) and 6(b) reveals important features of intramolecular energy flow and subsequent bond breaking and formation in the reaction taking place on a subpicosecond scale. For the representative trajectory considered in Figure 6, the reaction energy available for partitioning among various motions in the product state is 0.867 eV. The major portion of this energy deposits in the translational and vibrational motions of OH [i.e., in the limit $t \to +\infty$, $E_t(\infty) = 0.388$ eV and $E_v(\infty) = 0.285$ eV]. Only a small fraction is found to deposit in the rotational motion: $E_r(\infty) = 0.0017$ eV.

The ensemble-averaged energy transfer to the silicon surface $\langle E_s \rangle$ is 0.029 eV. Although this amount is not large, the bulk solid phase still shares a significant portion of the reaction exothermicity. The dissipation of energy to the heat bath is very slow compared to the reaction step that occurs

on a subpicosecond time scale. After breaking the O-Si bond, a portion of the reaction exothermicity deposited in the vibration of the zeroth Si rapidly propagates to the inner region of the $N+1$ atom chain, and then it slowly propagates into the heat bath governed by the friction term in Eq. (2d). Figure 6(c) shows the time evolution of the surface energy $E_s(t)$ for the representative trajectory with a reaction time of 0.17 ps at (1800, 300 K). The surface energy rapidly builds up on the impact but its dissipation into the heat bath is very slow. The time evolution shows the dissipation process continuing long after reaction. The dotted curve is for the nondissipative case in which the dissipation mechanism is suppressed so the energy remains in the chain. In this case, the energy gained from the reaction zone remains in the $(N+1)$-atom chain after the O-Si dissociation. The difference between these two energies in the limit $t \rightarrow \infty$ is the amount of energy transfer to the solid (0.192 eV). A model neglecting the participation of solid atoms to the reaction is found to be grossly inadequate.

Concluding Comments

We have studied the Eley-Rideal reaction of atomic hydrogen with chemisorbed oxygen atoms on a silicon surface in classical trajectory procedures. The reaction probability is essentially independent of the surface temperature between 0 and 700 K, whereas its dependence on the gas temperature is significant. All reactive events occur on a single collision via a strong interaction between the gas atom and the adatom, leading to the transfer of a large amount of energy to the adatom-surface bond on a subpicosecond scale. The distribution of reactive events is localized in the immediate region around the adatom site on the surface. Most of the reaction exothermicity deposits in the translational and vibrational motions of the product molecule and a smaller, but significant amount dissipates into the surface. The majority of OH molecules are produced in low-lying vibrational energy states sharing about 25% to 30% of the available energy. The vibrational population distribution is found to be statistical. The amount of energy shared by the rotational motion is much smaller, implying that OH rotation does not play an important role in the desorption process.

Acknowledgments. This study was financially supported by Special Research Program of Chonnam National University, 2009.

References

1. *Interaction of Atoms and Molecules with Solid Surfaces*; Bortolani, V., March, N. H., Tosi, M. P., Eds.; Plenum: 1990.
2. *Dynamics of Gas-Surface Interactions*; Rettner, C. T., Ashfold, M. N. R., Eds.; Royal Society of Chemistry: 1991.
3. Somorjai, G. A. *Introduction to Surface Chemistry and Catalysis*; Wiley: 1994.
4. Shustorovich, E. *Surf. Sci. Rep.* **1986**, *6*, 1.
5. Christmann, K. *Surf. Sci. Rep.* **1988**, *9*, 1.
6. *CRC Handbook of Chemistry and Physics*, 64th ed.; Weast, R. C., Ed.; CRC Press: 1983; pp F176-F181.
7. Koleske, D. D.; Gates, S. M.; Jackson, B. *J. Chem. Phys.* **1994**, *101*, 3301.
8. Kratzer, P. *J. Chem. Phys.* **1997**, *106*, 6752.
9. Buntin, S. A. *J. Chem. Phys.* **1998**, *108*, 1601.
10. Ree, J.; Shin, H. K. *J. Chem. Phys.* **1999**, *111*, 10261.
11. Kim, Y. H.; Ree, J.; Shin, H. K. *Chem. Phys. Lett.* **1999**, *314*, 1.
12. Wang, G. T.; Mui, C.; Musgrave, C. B.; Bent, S. F. *J. Phys. Chem. B* **1999**, *103*, 6803.
13. Kádas, K.; Molnár, L. F.; Náray-Szabó, G. *J. Mol. Struc.* (*Theochem*) **2000**, *501-502*, 459.
14. Zgierski, M. Z.; Smedarchina, Z. K. *Europhys. Lett.* **2003**, *63*, 556.
15. Skliar, D. B.; Willis, B. G. *J. Phys. Chem.* **2008**, *112*, 9434.
16. Cheng, C. C.; Lucas, S. R.; Gutleben, H.; Choyke, W. J.; Yates, J. T., Jr. *J. Am. Chem. Soc.* **1992**, *114*, 1249.
17. Yates, J. T.; Cheng, C. C.; Gao, Q.; Choyke, W. J. *Surf. Sci. Rep.* **1993**, *19*, 79.
18. Kim, Y. H.; Ree, J.; Shin, H. K. *J. Chem. Phys.* **1998**, *108*, 9821.
19. Adelman, S. A. *Adv. Chem. Phys.* **1980**, *44*, 143.
20. Ree, J.; Kim, Y. H.; Shin, H. K. *Chem. Phys. Lett.* **2002**, *353*, 368.
21. *American Institute of Physics Handbook*, 3rd ed.; Gray, D. E., Ed.; McGraw-Hill: 1972; pp 4-116.
22. Ree, J.; Kim, Y. H.; Shin, H. K. *J. Chem. Phys.* **1996**, *104*, 742.
23. Huber, K. P.; Herzberg, G. *Constants of Diatomic Molecules*; Van Nostrand Reinhold: 1979.
24. Jenichen, A.; Johansen, H. *Surf. Sci.* **1988**, *203*, 143.
25. Ghio, E.; Mattera, L.; Salvo, C.; Tommasini, F.; Valbusa, U. *J. Chem. Phys.* **1980,** *73*, 556
26. Lim, S.; Ree, J.; Kim, Y. H. *Bull. Kor. Chem. Soc.* **1999**, *20*, 1136.
27. Huffman, M.; McMillan, P. *J. Non-Cryst. Solids* **1985**, *76*, 369.
28. Krol, J. M.; Rabinovich, E. M. *J. Non-Cryst. Solids* **1986**, *82*, 143.
29. Park, J.; Ree, J.; Lee, S. K.; Kim, Y. H. *Bull. Kor. Chem. Soc.* **2007**, *28*, 2271.
30. Ree, J.; Kim, Y. H.; Shin, H. K. *J. Phys. Chem. A* **2003**, *107*, 5101.
31. Rogers, P. J.; Selco, J. I.; Rowland, F. S. *Chem. Phys. Lett.* **1983**, *97*, 313.
32. Rowland, F. S. *Faraday Discuss. Chem. Soc.* **1983**, *75*, 158.
33. Eaborn, C.; Jones, K. L.; Smith, J. D.; Tavakkoli, K. *J. Chem. Soc. Chem. Commun.* **1989**, *17*, 1201.
34. Lopez, V.; Marcus, R. A. *Chem. Phys. Lett.* **1982**, *93*, 232.
35. Marcus, R. A. *Faraday Discuss. Chem. Soc.* **1983**, *75*, 103.
36. Lopez, V.; Fairen, V.; Lederman, S. M.; Marcus, R. A. *J. Chem. Phys.* **1986**, *84*, 5494.
37. Shin, H. K. *J. Chem. Phys.* **1990**, *92*, 5223.
38. Gross, A. *Surf. Sci. Rep.* **1998**, *32*, 291.